Radiative neutron capture cross sections on ^{176}Lu at DANCE

O. Roig, M. Jandel, V. Méot, E. M. Bond, T. A. Bredeweg, A. J. Couture, R. C. Haight, A. L. Keksis, R. S. Rundberg, J. L. Ullmann, and D. J. Vieira

Phys. Rev. C **93**, 034602 — Published 3 March 2016

DOI: 10.1103/PhysRevC.93.034602

Radiative neutron capture cross sections on ^{176}Lu at DANCE

O. Roig,[1,*] M. Jandel,[2] V. Méot,[1] E.M. Bond,[2] T.A. Bredeweg,[2] A.J. Couture,[2] R.C Haight,[2] A.L. Keksis,[2] R.S. Rundberg,[2] J.L. Ullmann,[2] and D.J. Vieira[2]

[1] *CEA, DAM, DIF, F-91297 Arpajon, FRANCE*
[2] *Los Alamos National Laboratory, Los Alamos, New Mexico 87545, USA*

The cross section of the neutron capture reaction ^{176}Lu(n,γ) has been measured for a wide incident neutron energy range with the Detector for Advanced Neutron Capture Experiments at the Los Alamos Neutron Science Center. The thermal neutron capture cross section was determined to be (1967±137) b for one of the Lu natural isotopes, ^{176}Lu. The resonance part was measured and compared to the Mughabghab's atlas using the R-matrix code, SAMMY. At higher neutron energies the measured cross sections are compared to ENDF/B-VII.1, JEFF-3.2 and BRC evaluated nuclear data. The Maxwellian averaged cross sections in a stellar plasma for thermal energies between 5 keV and 100 keV were extracted using these data.

PACS numbers: 25.40.Lw, 28.20.Ka, 26.20.Kn, 27.70.+q
Keywords: radiative capture, Lutetium isotopes, DANCE, resonance paramaters, MACS

I. INTRODUCTION

Neutron capture cross sections are of high interest in nuclear astrophysics to investigate the s-process in which the synthesis of heavy elements is dominated by neutron induced reactions. The thermonuclear reaction rates needed for s-process nucleosynthesis are particularly amenable to experimental investigation as the s-process follows the valley of beta-stability, so most of the reactions take place on stable isotopes. In this landscape, specific isotopes are s-only nuclei, only produced by the s-process [1]. They provide insight to specific characteristics of this nucleosynthesis process. This is why many investigations were performed on Lutetium isotopes [2–5]. ^{175}Lu is an important so-called waiting point nuclei, having a comparatively long half-life with respect to β-decay time, while the s-only ^{176}Lu exhibits a thermally enhanced beta decay rate [6], making it a sensitive branch point for estimating neutron density and temperature at the nucleosynthesis site [7]. Macklin [8, 9], Beer [10, 11], Bokhovko [12] and Wisshak [5] performed various measurements on Lutetium isotopes in the neutron energy region of astrophysical interest between 3 keV and 200 keV.

In this context, the Maxwellian average cross sections (MACS) in a stellar plasma of thermal energy kT for such nuclei are crucial parameters to predict the evolution of the nucleosynthesis [13]. Calculating MACS for a set of stellar temperatures between 5 keV and 100 keV requires cross section values for a neutron energy range as wide as possible including the resolved resonance region [5]. The neutron capture reaction rates are usually obtained by measuring the neutron capture cross section using a neutron spectrum similar to a Maxwell-Boltzmann distribution at a given stellar temperature. The contribution of the resonance energy region to MACS is often determined by using the evaluated cross sections from data compilation as given by Kopecky [14]. For the ^{176}Lu isotope, resonance energies and neutron widths were obtained by Kalebin [15] in one important absolute measurement of transmission cross section up to 200 eV. These data are only overlapped by data up to 47 eV from Block [16], up to 12 eV from Vertebnyy [17] and up to 1.56 eV from Brunner [18] and Widder [19]. As the resonances at relatively high neutron energies could give a significant contribution to the low kT MACS, resonance energies, widths and cross sections are required parameters to accurately describe the s-process around these Lu isotopes. Information like resonance characterization, level densities, neutron widths, level spacings and γ-cascade description for odd-odd (^{176}Lu) nuclei could further constrain and improve reaction model calculations. It is particularly interesting for ^{176}Lu which is one of only two odd-odd rare earth isotope (the other is ^{138}La) and the highest ground state spin ($J^{\pi}=7^{-}$), that exists naturally ($t_{1/2} = 3.76 \times 10^{10}$ yr) on earth. This article focuses on the determination of the radiative capture cross section for ^{176}Lu from the thermal neutron energy to a few keV including the resonance energy region. Neutron capture measurement on ^{176}Lu has been undertaken using an isotopically enriched target, by combining the capabilities of the Los Alamos Neutron Scattering CEnter (LANSCE) and the DANCE array at the Los Alamos National Laboratory. Our measurements overlap and provide a valuable cross check of the recent measurements of Wisshak [5] in the 3 keV

*olivier.roig@cea.fr

and higher energy region. Finally new MACS using the resonance region cross sections measured in this work are presented for various stellar temperatures.

II. EXPERIMENTAL METHOD

A. The LANSCE facility

The LANSCE linac accelerator provides a 800 MeV proton beam. This beam is compressed using the proton storage ring (PSR) to a 250 ns pulse. A 100 μA beam is delivered at a rate of 20 Hz into the spallation neutron source [20], which is a tungsten target. The neutrons are moderated in a water moderator located in backscatter geometry just above the upper tungten target. The Detector for Advanced Neutron Capture Experiments (DANCE) [21] is located on the 20.25 m long flight path 14.

B. The DANCE array

The DANCE array is composed of 160 barium fluoride (BaF_2) scintillators. The nearly 4π geometry enables calorimetry by capturing all of the cascade γ rays from the reaction. High granularity, high neutron flux and high performance data acquisition enable measurements using small samples with masses of $\cong$1 mg and/or radioactive nuclides with an activity up to 1 GBq. For each γ-cascade following the neutron capture, the DANCE array provides the γ-sum energy, the multiplicity of crystal hit and the γ ray energies from each crystal. Taking into account the Compton effect inside the ball array, a cluster of hits is defined as where at least one neighboring crystal was also hit. Information is also provided as cluster multiplicty and cluster γ ray energies determined for each γ-cascade.

The sample is placed at the center of the DANCE array inside a beam tube under vacuum surrounded by a ^{6}LiH neutron-scattering shield. The 6 cm thick ^{6}LiH sphere attenuates scattered neutrons flux by a factor of about 100 for the highest neutron energies [22]. The target is assembled in a DANCE holder consisting of an aluminum cylinder container, a single ring where the sample foil is glued and a system to lock the sample target at the middle of the cylinder.

Both segmented and continuous modes of the DANCE acquisition [23] were used to accurately get each part of the neutron spectrum over the wide energy range. Segmented mode includes a $\gamma - \gamma$ coincidence in a time window of 200 ns with a γ threshold of about 150 keV used as a trigger. In this case, the acquisition system gets data with a fixed dead time of 3.4 μs over the 14 ms time-of-flight range thus including thermal neutron energy.

Continuous mode consists of two time-of-flight windows of 250 μs widths corresponding to the memory buffer of data collected with no dead time. The neutron energy range covered depends on the choice of both windows. Continuous mode is usually used for neutron energy above 8.5 eV.

C. The Lu target

A thin target of enriched ^{176}Lu was prepared by the CSNSM (Centre de Sciences Nucléaires et de Sciences de la Matière) laboratory in Orsay (France). A ^{176}Lu ion beam extracted by the electromagnetic isotope separator called Sidonie [24] was soft-landed at an energy about 50 keV onto a 1 μm thin aluminized mylar foil using a mask with a 7 mm diameter hole. A few atomic layers of Al were evaporated on the surface of the mylar to be conductive in order to allow the electrostatic deceleration of the ion beam. The isotopic purity reached with Sidonie was previously measured on a test foil using an instrumental neutron activation analysis (INAA) at Pierre Süe laboratory in Saclay. The isotopic ratio ^{175}Lu/^{176}Lu obtained is $(4.29\pm0.22)\times10^{-5}$ (99.9957$\pm$0.0002%). The total mass of the final target was obtained by two low-activity measurements at Los Alamos National Laboratory and at the PRISNA (Plateforme Régionale Interdisciplinaire de Spectrométrie Nucléaire en Aquitaine) facility in Bordeaux. The first gives 418$\pm$20 mBq and the second one 409$\pm$53($\pm$12 stat. $\pm$41 syst.) mBq. The areal density of the ^{176}Lu target is (1.854$\pm$ 0.076)$\times10^{-6}$ atoms/barn, then the mass is (208$\pm$10) μg. The homogeneity of the target was studied using x-ray fluorescence measurements at Los Alamos National Laboratory and found to be homogenous.

The Lu target was mounted on the standard DANCE aluminum holder. One blank (aluminized mylar backing foil without Lu) target was made with the same procedures to be able to subtract background effects.

D. Beam monitors

The neutron flux measurement was achieved at DANCE using a neutron beam monitor located 2.5 m from the DANCE target. The monitor used for present experiments was a BF_3 ionization chamber, LND 2231 model. This detector is based on the ^{10}B(n,α)^{7}Li reaction from which both products are detected. It is located 22.76 m away from the moderator, 2.5 m from DANCE. The neutron energy spectrum of the flight path 14 (FP14) was obtained from the beam monitor event rates using the ^{10}B(n,α)^{7}Li reaction cross section. Both neutron fluxes at the beam monitor position, ϕ^{BF_3}, and at the target position, ϕ, are related by the simple formula $\phi^{BF_3} = \alpha \times \phi$. The factor α includes the difference of the position between the BF_3 monitor and the target, and the unmeasured absolute efficiency of the beam monitor.

III. DATA ANALYSIS

A. General features

The (n,γ) cross section can be determined for a wide neutron energy range from the number of measured radiative capture events per eV. In order to extract only the desired reaction, here the ^{176}Lu (n,γ), the DANCE array allows for accuratetly selecting the γ-cascades following the formation of the compound nucleus after the neutron capture, through:

- a precise time selection of the γ-cascades to decrease uncorrelated γ rays;
- a total γ energy measurement of the γ-cascades, focusing on the detector response of the desired reaction avoiding background γ ray cascades from scattered neutrons capturing on Barium Fluoride (BaF_2) crystals. This value is called energy sum, E_{sum};
- a determination of the multiplicitiy of the γ-cascades, defining specifically the events of the desired reaction and avoiding fortuitous γ ray coincidences.

To optimize all these DANCE characteristics, one needs to properly prepare data and to carefully apply background subtraction and selection cuts. The data analysis consists in doing:

- a calibration for γ-energy;
- dead-time corrections for the segmented acquisition mode;
- a background subtraction and cuts.

A fully detailed data analysis for DANCE data can be found in Ref. [25].

B. Calibration

For γ energy calibration, various sources are used to calibrate BaF_2 crystals: ^{88}Y, ^{22}Na and ^{60}Co are the most commonly used sources at DANCE. The alpha intrinsic activity of BaF_2 crystals due to Radium, a chemical homologue of Barium, is used to follow and to correct calibration during the experiment. For that, a pulse shape discrimination is performed using the two components, fast and slow, of the signal coming from BaF_2 crystals. The alpha signals are removed in the analysis of the capture events and are only used for gain matching. The threshold for each BaF_2 crystals was set at 150 keV γ ray energy.

A neutron energy is determined by converting time using the flight path distance of about 20.25 m. A precise correction takes into account a delay time between the gamma flash from the spallation target hit by the proton beam, corresponding to the neutron emission, and the reference time, corresponding to the accelerator frequency. A time adjustement between crystals was performed in order to set a coincidence window as precise as $\pm$5 ns. From data extraction from acquired partial waveforms (fast components) and integrals (slow components), a code called FARE [26], specifically designed for the DANCE array, converts these data to physical observables (gamma ray energy, sum energy, cluster multiplicity, time-of-flight, flux).

C. Dead-time correction

Data were acquired using the segmented acquisition mode for the neutron energies between thermal neutron energy and keV region. The segmented mode is used with a dead time which is about 3.5 μs [23]. To correct for the dead time, we used a well-known technique in time-of-flight experiments by applying a simple analytic correction [27–29] using a 3.5 μs fixed dead time. A correction factor is extracted and applied to data. As it depends on the number of events per time unit, it is larger for energies corresponding to neutron resonances (see Fig. 1).

The relative variance of the proton beam current during each run was checked and found to be negligible. It was not used in the correction [27]. Details of the method can be found in Ref. [28] and Ref. [25]. Above 8.5 eV neutron energy, data were acquired using the deadtime free continuous acquisition mode. A cross-check between the deadtime corrected data (segmented mode) and the deadtime free data (continuous mode) shows a very good agreement. Fig. 2 presents the comparison between the data acquired in segmented mode after deadtime correction and in continuous mode without any correction.

D. Background subtraction

Neutrons from the beam are scattered by the backing foil, the DANCE target holder and the target itself. In spite of the shielding of the ^{6}LiH shell, some neutrons go across the ^{6}LiH shell and interact with the BaF_2 crystals causing a relatively important γ ray background. The total γ ray energy left in DANCE is quite different between ^{176}Lu reactions (Q-value = 7072.9 keV) and some of Ba isotopes, ^{135,137}Ba (Q-value = 9107.74 keV, 8611.72 keV), to distinguish between both elements. But for ^{134,136,138}Ba (Q-value = 6971.97 keV, 6905.63 keV, 4723.43 keV), we need to use a blank target composed of a backing foil without Lutetium to properly estimate the contribution of these scattered neutrons. A normalization between the yield from the blank and ^{176}Lu targets is achieved on the total γ energy measurement for the γ-cascades of the ^{135,137}Ba isotopes which have Q-values higher than the ^{176}Lu one.

E. Raw data reduction

Two main parameters are crucial to reduce DANCE data: Multiplicity and Energy sum, E_{sum}. Multiplicity information from DANCE array allows the reduction of background events. Multiplicity cut is a selection of the number of clusters (group of adjacent hit BaF_2 crystals) which represents the number of γ rays in the γ cascades following the neutron capture by the ^{176}Lu nucleus. As a perfect E_{sum} spectrum (without the DANCE detector response function) would represent the Q_{value} of the (n,γ) reaction on a nucleus plus the incident neutron kinetic energy minus the recoil energy of the nucleus, a E_{sum} selection, called also the Q_{gate} cut, was used in addition to the multiplicity cut. A specific signal-to-noise study for ^{176}Lu target was performed to find the best solution to reduce background through multiplicity information and cuts on the total γ ray energy. The determination of event selection conditions was achieved and is presented in Table I. A $\pm$5 ns coincidence window for γ rays was also used to select more precisely each γ-cascade event.

IV. RESULTS AND DISCUSSION

The neutron capture cross sections on ^{176}Lu was obtained from the neutron thermal energy up to a few hundred keV. Each part of this large energy range has been carefully studied to obtain information to compare with existing data or reaction models. The first study gives the thermal cross section measured at DANCE. The second study looks at the resonance energy range. The third study is related to the keV region comparing these new results to the previous results and the evaluated data from ENDF/B-VII [30], JEFF-3.2 [31] and BRC (Bruyères-le-Châtel evaluation) [32] data bases. The last study presents the calculation of the Maxwell averaged cross sections (MACS) for various stellar temperatures related to s-process for some astrophysical sites.

A. Normalized Capture Yield

The capture yield is defined as the number of capture events divided by the neutron flux hitting the target at a given energy. Here, the capture yield is normalized to data including resonance parameters from the Atlas of resonances by S.F. Mughaghab [33]. The normalization includes the alpha parameter mentioned in Sec. II D, the

DANCE detection efficiency and the effect of data reduction. The normalization point was chosen on the resonance at 1.565 eV. The neutron and gamma widths of this well-known resonance are given with uncertainties better than 1% and 2%, respectively. Figure 3 presents the capture yield from data and the fit from the SAMMY code to determine the normalization factor on the resonance capture yield at 1.565 eV. The moderated broadening function which is used in the SAMMY code for the DANCE flight path is the Renseselaer Polytechnic Intstitute broadening function (RPI). The 39 RPI resolution parameters have been studied by P. Koehler et al. [34]. Figure 4 shows the capture yield from the DANCE data for the ^{176}Lu(n,γ) reaction, normalized at 1.565 eV.The binning energy used here is 0.1% from thermal energy to 100 eV, 1% to 1 keV and 10% to 100 keV.

1. Cross section at thermal neutron energy

The measurement of the thermal radiative capture cross section measured using the time-of-flight method was achieved by Widder [19] using a Moxon-Rae detector and by Baston [37] extracting it from total cross section.

In this work, the measured thermal neutron capture cross section on ^{176}Lu using DANCE is determined, from the SAMMY fit, to be 1967±137 b (5.7% uncertainty on DANCE capture yield and 4% uncertainty on the neutron flux) at the neutron energy 0.0253 eV using the time-of-flight technique. This value is obtained from the normalized measurement using the yield, the neutron flux and the target mass. A correction of about +4.5% obtained from Fig. 1 is applied to correct the deadtime due to the segmented acquisition mode in this neutron energy region. Figure 5 shows the comparison between radiative capture cross sections on ^{176}Lu at the neutron energy 0.0253 eV measured by the time-of-flight measurements or in a thermal neutron flux by activation. Fig. 5 shows Mughaghab compilation values [36],[33] which were re-evaluated in 2007. The current Mughabghab ^{176}Lu(n,γ) neutron capture cross section is 2020±70 b at E_n=0.0253 eV. ENDF/B-VII.1, JEFF-3.1 and JENDL-3.3 evaluations use 2097 b as thermal neutron capture cross section for ^{176}Lu(n,γ) reaction.

2. Resonance region up to 400 eV

The capture yields for the resonance region are presented in Fig. 6. All resonances referenced in the literature [33] are observed with some new ones above 135 eV. A comparison between DANCE data and the capture yield reconstructed from these known resonance parameters is achieved. We can notice that the energy of some resonances could be redefined. We checked that the time-of-flight t_0 related to the path of flight L_0 is well defined in this experiment. The time-of-flight was corrected by an addition of δt=-523 ns, coming from the difference between the γ-flash when protons impinging the spallation target and the reference clock T_0, given by the PSR. A fine adjustment of the flight path value was performed using a SAMMY fit of data. The flight path was set to 20.255 m. The resolution function applied is given in Sec. IV A. The resonance parameters of the ^{176}Lu(n,γ) were determined by few sets of data from: Kalebin [15] up to 136 eV, Block [16] up to 46.7 eV, Vertebnyy [17] and Foote [40] up to 15 eV, Wider [19] from thermal neutron energy to 1.9 eV, and Brunner [18] for two first resonances.

The SAMMY code has been used to extract all the resonance parameters up to 400 eV as Table II presents. An assignment of spin, 13/2 or 15/2, of the reached state in the ^{177}Lu compound nucleus, was performed using the SUGGEL code [41] determining the most probable value depending on the gΓ_n where $\Gamma_n$is the neutron width, g is the spin statistical factor (7/16 for a spin 13/2 and 9/16 for a spin 15/2). Several iterations of the SAMMY analysis give a determination of the resonance energy and parameters. Table II presents theses results. Table III and Table V give results for new resonances above 135 eV up to few hundred eV.

The orbital momentum assignment l of every resonances was checked using the definition of the strength function for various partial waves to obtain the expected values,

$$< g\Gamma_n^l/\sqrt{E} >= (2l+1)V_l S_l D_l \quad (1)$$

for s-waves (l=0) and p-waves (l=1). V_l is the penetrability for a square well potential given by S.F. Mughabghab [33]. S_l is the neutron strength function. D_l is the level spacing. Fig. 7 shows these expected values for s and p waves using the following values: S_0=1.61×10^{-4}, D_0=1.6 eV, S_1=1.7×10^{-4} [33]. D_1 is deduced from D_0 using the SUGGEL code [41]. Fig. 7 demonstrates that only s-waves are seen in this neutron energy range.

3. Statistical analysis of resonances

A new set of resonance parameters is used to determine new values of the level spacing D_0 and the neutron s-wave strength function S_0. A careful analysis of the new resonance parameters above 136 eV was achieved using the SAMDIST code [42]. We checked the coherence of this new set of resonance parameters according to the Dyson-Metha statistics [43], the Wigner distribution for the level spacing, the Porter-Thomas distribution for the neutron widths [44] and the χ^2 law for the gamma widths.

A reliable approach to determine the averaged level spacing D_0 for s-waves is based on neutron widths and the number of resonances observed in the neutron energy range ΔE. The formula used is extracted from the Gaussian orthogonal ensemble (GOE), a statistical model for the compound nucleus initiated by E. Wigner. A complete overview of the theory of GOE can be found in Ref. [45] and references therein. Here we use the fact that the number of levels, $N(x_t)$, with a reduced neutron width, $\Gamma_n^0=\Gamma_n/\sqrt(E_0)$, larger than a threshold defined by $x_t = g\Gamma_{n,t}^0/ < g\Gamma_{n,t}^0 >$, can be determined by the following formula:

$$N(x_t) = N_0(1 - erf(\sqrt(x_t)) \tag{2}$$

where N_0 is the total number of levels (observed and missing), $< g\Gamma_{n,t}^0 >$ the average reduced neutron width in the ΔE range that we consider and erf(x) the Gauss error function. Fig. 8 shows this function fitted on the DANCE data for the ^{176}Lu(n,γ) reaction. All resonances below the limit of x_t=4×10^{-2} cannot be observed in our experiment and are not included in this analysis. Then N_0 is found to be 181 by extrapolating the function to zero threshold instead of 144 observed levels in the neutron energy range up to 400 eV. The uncertainty of N_0 was determined by moving around the latter limit. We can deduce the averaged level spacing $D_0=\Delta E/N_0$=(2.20±0.02) eV for the energy range from thermal neutron energy up to 400 eV. This value is compared to D_0=(1.61±0.16) eV in literature [33] obtained from an energy range up to 136 eV only.

The reference input parameter library, RIPL2 [46], gives values from various levels density models. Tab. IV presents the values compared to our estimated value. A good agreement is found.

From this new set of resonance parameters, we can extract a new value of the neutron strength function, S_0. For all s-waves, S_0 is defined by the following formula:

$$S_0 = \frac{< g\Gamma_n^0 >}{< D_0 >} = \frac{1}{\Delta E}\sum g\Gamma_n^0 \tag{3}$$

The cumulative sum of the reduced neutron width was calculated for all s-wave resonances observed in this analysis up to a neutron energy of 400 eV. Fig. 9 shows the cumulative sum as a function of neutron energy in the upper pannel and the corresponding value of S_0 calculated at each neutron energy interval in the lower pannel. The peak at 135 eV is due to two resonances previously observed and also obtained here with large neutron widths. A linear fit of the upper curve from 60 eV up to 400 eV, gives directly the value of S_0, found to be (1.62±0.10) ×10^{-4}. This value is in agreement with S_0=(1.6±0.2)×10^{-4} from Ref.[33].

4. keV neutron energy region

Data for the ^{176}Lu(n,γ) reaction in the keV region were compared to the Hauser-Feshbach statistical calculations.

Fig. 10 shows the measured cross section on ^{176}Lu between 500 eV and 20 keV compared with the evaluated data from ENDF/B-VII.1. [30], JEFF-3.2 [31] and BRC [32]. This DANCE normalized measurement of ^{176}Lu capture cross section agrees well with previous data from H. Beer [11], K. Wisshak [5] and the evaluated cross sections.

5. Maxwellian-averaged (n,γ) cross sections

The Maxwellian-averaged neutron capture cross sections (MACS) are usually obtained by measuring the neutron capture cross section using a neutron spectrum similar to a Maxwell-Boltzmann distribution at a given stellar temperature [5]. In this work, having obtained a complete set of neutron capture cross sections on ^{176}Lu, MACS for stellar temperature between 5 keV and 100 keV can be extracted. The Maxwellian-averaged (n,γ) cross sections (MACS) in a stellar plasma of thermal energy kT is defined as in Ref.[48] by formula 4.

$$\left\langle \sigma\left(E\right)\sqrt{E}\right\rangle_{kT} = \int_0^\infty \sigma\left(E\right) E \frac{2e^{-E/kT}}{\sqrt{\pi}(kT)^2} dE \tag{4}$$

For ^{176}Lu, the MACS can be determined using three set of data. The first set is the DANCE data from thermal energy to 3 keV (resonance region). The other two sets are taken from Ref.[5]: one is a measurement between 3 keV and 200 keV and the other one is from calculation up to 1 MeV. The calculated MACS resulting for the ^{176}Lu(n,γ) reaction at various kT values is given in Table VI and details in Table VII. The DANCE results at stellar temperature $\leq$ 15keV with resonances up to 900 eV are quite different from Ref.[5] where the highest resonance energies of ^{176}Lu were around 130 eV.

At higher stellar temperatures, above 30 keV, the DANCE MACS are different to those given in [5]. This discrepancy is essentially explained by a factor up to 1.8 higher between I3 integrals (see Tab.VII and Tab.VIII in [5]). This comes from the difference found between JEF-2.2 evaluation data used in [5, 14] and JEFF-3.2 and the data evaluation ENDF/B-VII.1 [30] and BRC [32] used here. The difference between evaluation data comes from the parametrisation of the optical potential. The fraction of the cross section due to the resonance region is presented in Table VI. As expected, the resonance region has an increasing influence at low temperatures. Taking into account accurately the resonance region changes the MACS. For some astrophysical sites, changing the MACS for the ^{176}Lu case could have a significant impact at low stellar temperature on the s-process nucleosynthesis as it is well described by M. Heil *et al.* in Ref. [50]. Nevertheless, at 30 keV stellar temperature, the total MACS value found for the ^{176}Lu(n,γ) reaction in this work is 1647$\pm$5 mb which is still in agreement with the KADONIS [51, 52] adopted value from [5], 1639$\pm$14 mb, and relatively higher than Bao's value, 1532$\pm$69 mb [13].

B. Conclusion

For the first time, over a large neutron energy range, the radiative neutron capture cross sections on the ^{176}Lu isotope was obtained. A complete and coherent set of resonance parameters was extracted up to 400 eV neutron energy. Some resonance energies were given up to 900 eV. The radiative capture cross sections were measured in the keV region and provided a valuable cross-checks with the previous data of Wisshak [5]. Level spacing D_0 was estimated to be D_0=(2.20$\pm$0.02) eV. A new value of the s-wave neutron strength function was determined to be (1.62$\pm$0.10) $\times 10^{-4}$. The evaluated data for the ^{176}Lu can reproduce our measurements. The Maxwellian-averaged (n,γ) cross sections are slightly different at low stellar temperature and in good agreement at higher stellar temperature with the results of Wisshak [5].

V. ACKNOWLEDGMENTS

The authors would like to thank P. Romain and B. Morillon from CEA, DAM, DIF for providing us their data evaluation. We would like to thank R.S. Rundberg from LANL and Ph. Hubert from CENBG (Bordeaux), independently, for their precise measurement of the low-activity of our target. This work has benefited from the use of the Lujan Center at the Los Alamos Neutron Science Center, funded by the DOE Office of Basic Energy Sciences and Los Alamos National Laboratory funded by the Department of Energy under contract W-7405-ENG-36. One of us (O.R.) is grateful to the Los Alamos National Laboratory and the Commissariat à l'Energie Atomique et aux énergies alternatives for support during his extended stay in Los Alamos and to the C-NR team and the DANCE collaboration for their warm hospitality.

[1] E. Anders and N. Grevesse, Geochim. Cosmochim. Acta **53**, 197 (1989).
[2] H. Beer, F. Käppeler, K. Wisshak, and R. Ward, Astrophys. J. Suppl. Series **46**, 295 (1981).
[3] M.A. Garner, D.G. Gardner, and R.W. Hoff, J. Phys. G: Nucl. Phys. **14**, S315 (1988).
[4] J.J. Carroll, J.A. Anderson, J.W. Glesener, C.D. Eberhard, and C.B. Collins, Astrophys. J. **344**, 454 (1989).
[5] K. Wisshak, F. Voss, F. Käppeler, and L. Kazakov, Phys. Rev. C **73**, 015807 (2006).
[6] K. Takahashi and K. Yokoi, At. Data Nucl. Data Tables **36**, 375 (1987).
[7] N. Klay, F. Käppeler, H. Beer, and G. Schatz, Phys. Rev. C **44**, 2839 (1991).
[8] R. Macklin and J. Gibbons, Phys. Rev. **159**, 1007 (1967).
[9] R.L. Macklin, D.M. Drake, and J.J. Malanify, Los Alamos Scientific Lab. Reports 7479, Los Alamos National Laboratory (1978).
[10] H. Beer and F. Käppeler, Phys. Rev. C **21**, 534 (1980).
[11] H. Beer, G. Walter, R.L. Macklin, and P.J. Patchett, Phys. Rev. C **30**, 464 (1984).
[12] M.V. Bokhovko, V.N. Kononov, N.S. Rabotnov, A.A. Voevodskiy, G.N. Manturov, and V.M. Timokhov, Obninsk Reports FEI 2169, Fiziko Energetscheskij Institut (1991).

[13] Z.Y. Bao, H. Beer, F. Käppeler, F. Voss, K. Wisshak, and T. Rauscher, At. Data Nucl. Data Tables **76**, 70 (2000).

[14] J. Kopecky, J.-Ch. Sublet, J.A. Simpson, R.A. Forrest, and D. Nierop, Report INDC(NDS)- 362, IAEA (1997), http://www-nds.iaea.org/reports-new/ indc-reports/indc-nds/indc-nds-0362.pdf.

[15] S.M. Kalebin, V.S. Artamonov, R.N. Ivanov, G.V. Rukolajne, T.S. Belanova, A.G. Kolesov, and V.A. Poruchikov, At.Energ. **42**, 506 (1977).

[16] R.C. Block, G.G. Slaughter, and J.A. Harvey, ORNL Reports ORNL 2718, Oak Ridge National Lab. (1959).

[17] V.P. Vertebnyy, P.N. Vorona, A.I. Kalchenko, V.G. Krivenko, L.E. Chervonnaya, and V.Yu Chervyakov, in *Proceedings of Int. Conf. on Neutron Physics* (1987), 2, p. 204.

[18] J. Brunner and F. Widder, in *Proceedibgs of Nuclear Data for Reactors conference* (1966), vol. 1, p. 61, https://www-nds.iaea.org/publications/indc/indc-iae%25A0034uvol.i/.

[19] F. Widder, Reports EIR-217, Eidg. Inst. Reaktorforsch., Wuerenlingen (1975).

[20] A. Michaudon and S. Wender, LANL Report LA-UR-90-4355, Los Alamos National Laboratory (1990), http://lib-www.lanl.gov/cgi-bin/getfile?00328726.pdf.

[21] R. Reifarth, T. Bredeweg, A. Alpizar-Vicente, J. Browne, E.-I. Esch, U. Greife, R. Haight, R. Hatarik, A. Kronenberg, J. O'Donnell, et al., Nucl. Instrum. and Meth. A **531**, 530 (2004).

[22] M. Heil, R. Reifarth, M.M. Fowler, R.C. Haight, F. Käppeler, R.S. Rundberg, E.H. Seabury, J.L. Ullmann, J.B. Wilhelmy, K. Wisshak, Nucl. Instrum. Methods Phys. Res., Sect. A **459**, 229 (2001).

[23] J. M. Wouters, A.A. Vicente, T.A. Bredeweg, E. Esch, R.C. Haight, R. Hatarik, J.M. O'Donnell, R. Reifarth, R.S. Rundberg, J.M. Schwantes *et al.*, IEEE Trans. Nucl. Sci. **53**, 880 (2006).

[24] N. Chauvin, F. Dayras, D. Le Du, and R. Meunier, Nucl. Instrum. and Meth. A **521**, 149 (2004).

[25] M. Jandel, T.A Bredeweg, E.M. Bond, M.B. Chadwick, R.R. Clement, A.J. Couture, J.M. O'Donnell, R.C. Haight, T. Kawano, R. Reifarth *et al.*, Phys. Rev. C **78**, 034609 (2008).

[26] M. Jandel, Todd A. Bredeweg, A. Couture, J. M. O'Donnell, J. L. Ullmann, LANL Reports LA-UR-12-21171, Los Alamos National Lab. (2012).

[27] C. Bowman and R. Bramblett, Report LINAC- 21, Lawrence Livermore National Laboratory (1962).

[28] M. Moore, Nucl. Instrum. Methods **169**, 245 (1980).

[29] P. Coates, Rev. Sci. Instrum. **63**, 2084 (1992), http://link.aip.org/link/?RSINAK/63/2084/1.

[30] M.B. Chadwick, M. Herman, P. Oblozinsky, M.E. Dunn, Y. Danon, A.C. Kahler, D.L. Smith, B. Pritychenko, G. Arbanas, *et al*, Nucl. Data Sheets **112**, 2887 (2011).

[31] T. J. collaboration, *Jeff-3.2: Evaluated nuclear data library.*, `https://www.oecd-nea.org/dbforms/data/eva/evatapes/jeff_32/` (March 5, 2014).

[32] P. Romain and B. Morillon, Private communication, CEA (2014).

[33] S. F. Mughabghab, *Atlas of neutron resonances* (Elsevier Science, 2007).

[34] P. E. Koehler, J. L. Ullmann, T. A. Bredeweg, J. M. O'Donnell, R. Reifarth, R. S. Rundberg, D. J. Vieira, and J. M. Wouters, Phys. Rev. C **76**, 025804 (2007).

[35] N. M. Larson, ORNL/TM- 9179/R7, Oak Ridge National Laboratory (2006), http://www.ornl.gov/sci/nuclear_science_technology/nuclear_data/sammy.

[36] S. F. Mughabghab, *Neutron Cross Sections* **1** (Academic Press, INC., 1984).

[37] A.H. Baston, J.C. Lisle, and G.S.G. Tuckey, J. Nucl. Energy, Part A: Reactor Science **13**, 35 (1960).

[38] P. S. D. Albert, Journal Kernenergie **10**, 306 (1967).

[39] T.E. Young, Prog.Rep.: U.S.AEC Nucl.Cross Sections Advisory Comm. Repts 33, Idaho National Laboratory (1970).

[40] H. Foote, H. Landon, and V. Sailor, Phys. Rev. **92**, 656 (1953).

[41] S. Oh and L. Leal, ORNL/TM- 2000-314, Oak Ridge National Laboratory (2001), https://www.osti.gov/scitech/biblio/777661.

[42] L. Leal and N. Larson, ORNL/TM- 13092, Oak Ridge National Laboratory (1995), https://www.osti.gov/scitech/biblio/130670.

[43] F.J. Dyson and M.L. Mehta, J. Math. Phys. **4**, 701 (1963).

[44] C. E. Porter and R. G. Thomas, Phys. Rev. **104**, 483 (1956).

[45] M. L. Mehta, *Random matrices* (Academic Press (New York, San Diego), 1991).

[46] T. Belgya, O. Bersillon, R. Capote, T. Fukahori, G. Zhigang, S. Goriely, M. Herman, A.V. Ignatyuk, S. Kailas, A. Koning, P. Oblozinsky, V. Plujko and P. Young, IAEA-TECDOC IAEA-TECDOC-1506, IAEA (2006), http://www-nds.iaea.org/RIPL-2/.

[47] S. S. et al, *Low Energy Neutrons and their Interaction with Nuclei and Matter*, vol. 16B (Ed. H.Schopper, Springer-Verlag, Berlin, 2000).

[48] R. Macklin and J. Gibbons, Rev. Mod. Phys. **37**, 166 (1965).

[49] B. Pritychenko and S. Mughabghab, Nucl. Data Sheets **113**, 3120 (2012).

[50] M. Heil, N. Winckler, S. Dababneh, F. Kppeler, K. Wisshak, S. Bisterzo, R. Gallino, A. M. Davis, and T. Rauscher, The Astrophysical Journal **673**, 434 (2008), URL `http://stacks.iop.org/0004-637X/673/i=1/a=434`.

[51] I. Dillmann, R. Plag, F. Käppeler, T. Rauscher , *The karlsruhe astrophysical database of nucleosynthesis in stars*, http://www.kadonis.org (Last modification: August 2009).

[52] I. Dillmann, M. Heil, F. Käppeler, R. Plag, T. Rauscher, F.-K. Thielmann, in *Proceedings of 12th International Symposium on Capture Gamma-ray Spectroscopy and related topics:* (2006), vol. 819, pp. 123–127.

Figures

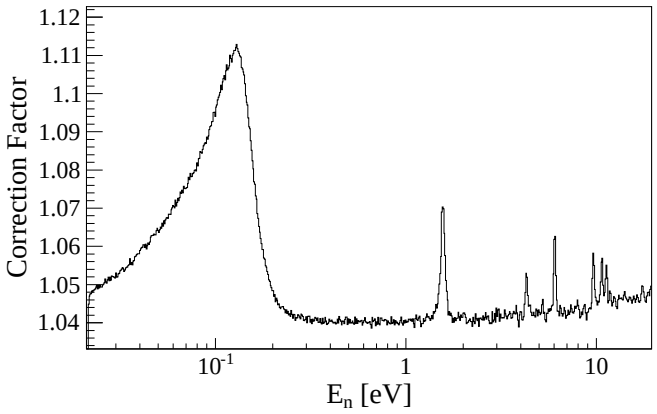

FIG. 1: Correction factor calculated from formula in [28] and applied to data taken in the segmented acquisition mode.

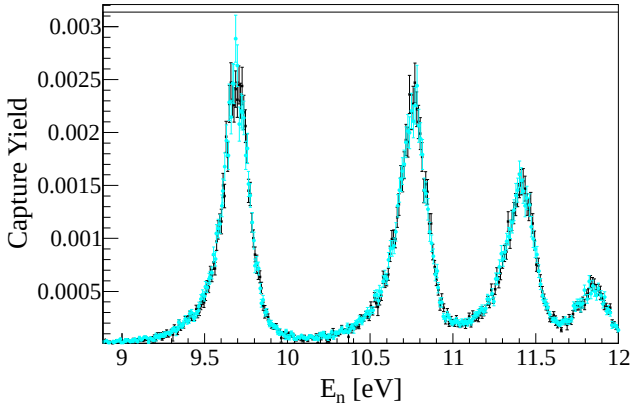

FIG. 2: (Color online) Comparison of the capture yield obtained from data acquired in segmented mode, the cyan (light gray) line, and in continuous mode, the black line. The segmented mode needs a deadtime correction performed using the analytic method given in [27–29].

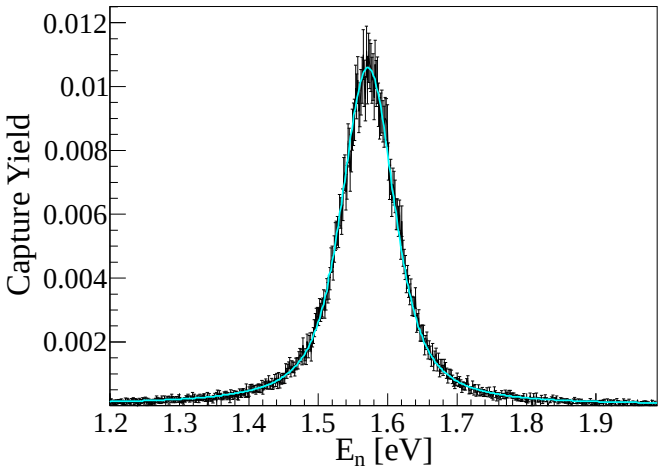

FIG. 3: (Color online) Normalized capture yield for the ^{176}Lu(n,γ) reaction using the R-Matrix code, SAMMY [35]. The fit of SAMMY is represented by the cyan (light gray) line.

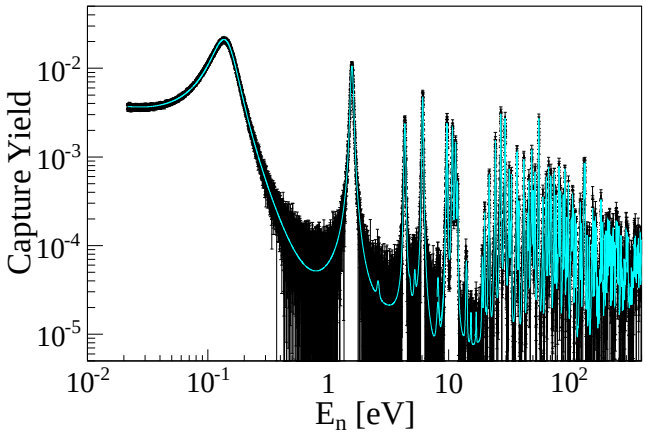

FIG. 4: (Color online) Normalized capture yield for the ^{176}Lu(n,γ) reaction and a fit, the cyan (light gray) line, of the R-Matrix code, SAMMY [35].

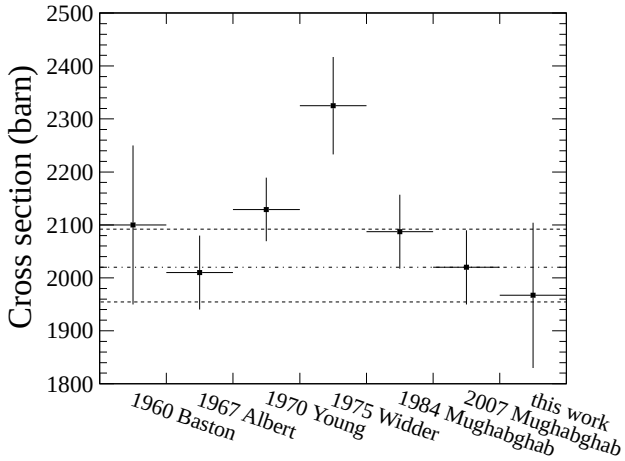

FIG. 5: (Color online) Some thermal neutron capture cross sections on ^{176}Lu from Baston [37], Albert [38], Young [39], Mughabghab [36], [33] and this work. The dotted lines represent limits from the errors of the last reference Mughaghab compilation value [33].

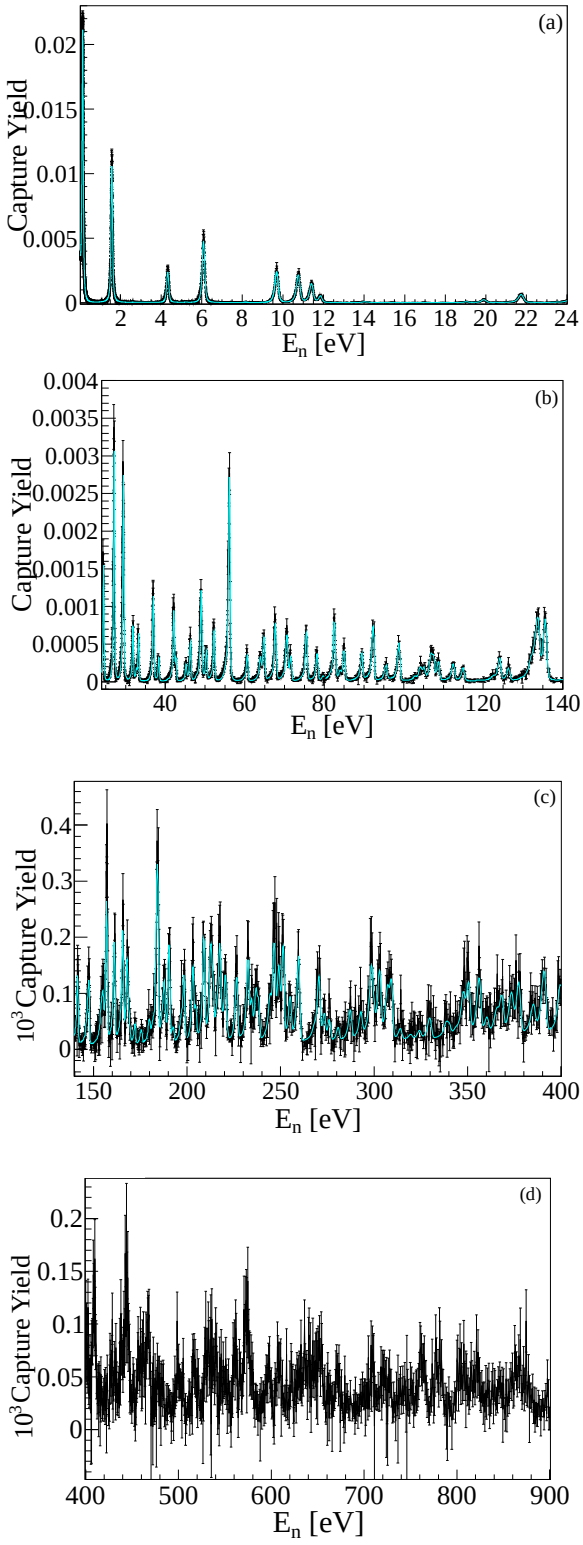

FIG. 6: (Color online) Radiative capture yield of the ^{176}Lu(n,γ) in the resonance energy range. The cyan (light gray) lines are the fit obtained using the SAMMY code [35].

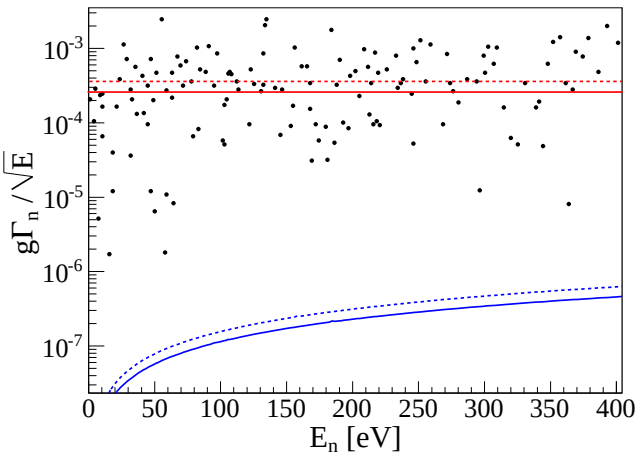

FIG. 7: (Color online) Expected values of $<g\Gamma_n/\sqrt{E}>$ for s-waves, the red (upper) line, and p-waves, the blue (lower) line [33]. Black circles represent resonance parameters extracted from the DANCE data for the ^{176}Lu(n,γ) reaction. Dotted lines are for DANCE values of $<g\Gamma_n/\sqrt{E}>$ determined in this work, respectively for s-waves (upper line) and p-waves (lower line).

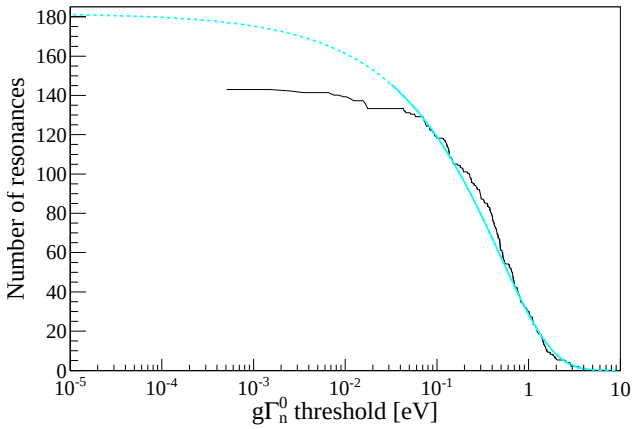

FIG. 8: (Color online) Number of observed resonances whose reduced neutron width is larger than a threshold as a function of this threshold. Resonances observed in the DANCE experiment are shown by the black line. The cyan (light gray) line represents a fit using formula 2. The extrapolated curve (dotted line) indicates the real number of levels, $N_0 = N(x_t = 0)$.

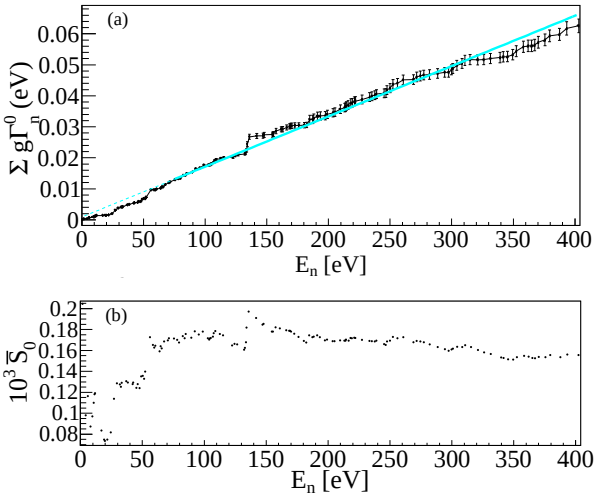

FIG. 9: (Color online) The cumulative sum of the reduced neutron widths as a function of neutron energy is shown in panel (a). The cyan (light gray) line is the fit using formula 3. The averaged value of $< S_0 >$ calculated from the cumulative sum up to a neutron energy is presented in panel (b).

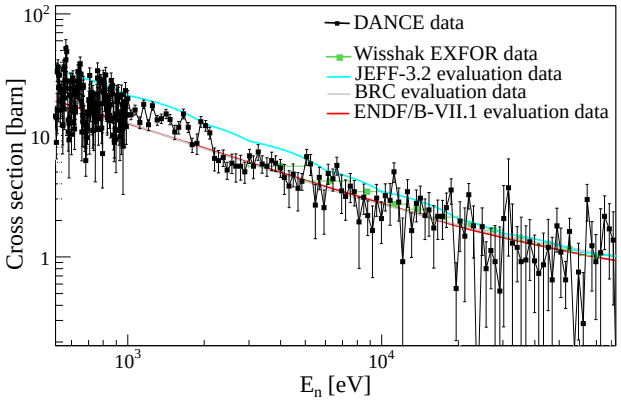

FIG. 10: (Color online) Neutron capture cross section on ^{176}Lu in the 0.5 to 70 keV region. These DANCE data (the black square), are compared to the previous measurements of Wisshak [5] [the green square (gray)], and recent data evaluations: JEFF-3.2 [31] [the cyan (upper) line], BRC [32] [the light gray line], and ENDF/B-VII.1 [30] [the red (dark gray) line].

Tables

TABLE I: Optimal data selection conditions for ^{176}Lu

Isotopes	Q-value (keV)	Q_{gate} cut (MeV)	Multiplicity cut
^{176}Lu	7072.99 (0.16)	[4.2, 7.3]	M≥4

TABLE II: Resonance parameters up to 140 eV neutron energy for ^{176}Lu(n,γ) reaction.

Mughabghab (2007)			This work			
Energy (eV)	Γ_γ (meV)	$2g\Gamma_n$ (meV)	J	Energy (eV)	Γ_γ (meV)	$2g\Gamma_n$ (meV)
0.1413 (1)	60.02 (150)	0.0865 (4)	13/2	0.13791 (1)	66(1)	0.0872 (2)
1.565 (4)	59 (1)	0.517 (5)	15/2	1.5694 (3)	59.1 (9)	0.516 (4)
4.36 (1)	64 (4)	0.43 (2)	15/2	4.316 (1)	66 (3)	0.424 (9)
6.130 (14)	59 (4)	1.46 (14)	15/2	6.072 (1)	69 (3)	1.40 (2)
8.14 (2)	177 (17)	0.0287 (16)	*	*	*	*
9.73 (3)	68 (2)	1.370 (12)	15/2	9.667 (1)	74 (3)	1.40 (2)
10.79 (4)	72 (2)	1.600 (17)	15/2	10.735 (1)	66 (5)	1.60 (4)
11.44 (4)	68 (8)	1.072 (73)	13/2	11.381 (2)	82 (5)	1.099 (18)
11.88 (5)	69 (8)	0.442 (15)	15/2	11.820 (3)	73 (8)	0.439 (15)
16.90 (7)	277 (17)	0.052 (7)	13/2	16.92 (5)	100 (103)	0.014 (6)
19.06 (7)	129 (14)	0.139 (6)	15/2	19.00 (1)	66 (28)	0.103 (15)
19.94 (7)	86 (7)	0.410 (9)	13/2	19.861 (5)	74 (13)	0.35 (2)
21.76 (8)	73 (5)	1.38 (5)	15/2	21.690 (4)	107 (8)	1.50 (3)
24.49 (10)	82 (7)	3.52 (7)	13/2	24.420 (3)	70 (5)	3.67 (7)
27.15 (11)	86 (15)	11.00 (16)	15/2	27.084 (3)	84 (5)	11.3 (2)
29.34 (12)	57 (32)	2.25 (138)	13/2	29.365 (4)	46 (5)	7.6 (2)
29.53 (12)	184 (47)	3.28 (115)	*	*	*	*
31.83 (14)	133 (15)	2.55 (10)	13/2	31.791 (5)	97 (11)	3.09 (8)
32.66 (14)	46 (22)	0.35 (4)	15/2	32.65 (2)	74 (41)	0.40 (5)
33.25 (14)	83 (10)	2.70 (17)	15/2	33.216 (5)	65 (10)	2.33 (7)
36.97 (15)	-	5.3 (11)	13/2	36.927 (5)	106 (9)	6.54 (15)
38.30 (15)	-	1.76 (60)	13/2	38.294 (8)	55 (15)	1.61 (6)
42.06 (16)	56 (12)	5.66 (54)	15/2	42.079 (7)	85 (17)	5.50 (17)
42.55 (16)	-	1.46 (12)	13/2	42.62 (1)	52 (30)	1.72 (13)
45.13 (17)	115 (27)	1.49 (5)	15/2	45.16 (1)	85 (33)	1.24 (8)
46.22 (17)	86 (22)	3.66 (26)	13/2	46.256 (7)	87 (16)	4.11 (14)
47.80 (17)	-	0.08 (4)	15/2	47.76 (7)	106 (83)	0.16 (5)
49.02 (18)	-	11.2 (50)	15/2	48.976 (6)	105 (14)	9.9 (3)
50.13 (18)	-	3.0 (16)	15/2	50.28 (2)	91 (25)	2.8 (2)
51.35 (18)	-	0.15 (6)	13/2	51.4 (1)	96 (83)	0.09 (7)
52.13 (18)	145 (31)	4.57 (25)	13/2	52.212 (7)	107 (15)	6.7 (2)
55.98 (18)	-	28.9 (34)	15/2	56.076 (6)	70 (8)	35.9 (13)
58.54 (18)	-	0.49 (11)	13/2	58.60 (9)	70 (71)	0.03 (2)
59.63 (18)	-	0.27 (8)	15/2	59.65 (9)	110 (86)	0.17 (6)
60.68 (18)	-	6.7 (8)	13/2	60.56 (1)	79 (22)	4.1 (2)
64.02 (19)	-	3.4 (5)	15/2	63.89 (2)	104 (48)	3.3 (4)
64.96 (19)	-	4.6 (6)	13/2	64.80 (2)	76 (24)	7.5 (5)
65.84 (19)	-	0.13 (6)	15/2	65.8 (2)	91 (81)	0.13 (11)
67.81 (19)	-	12.0 (16)	13/2	67.65 (1)	118 (20)	12.5 (4)
70.6 (2)	-	19.1 (21)	15/2	70.55 (1)	182 (37)	9.6 (4)
71.6 (2)	-	8.3 (13)	13/2	71.52 (2)	84 (33)	5.2 (4)
75.6 (2)	-	13.4 (16)	15/2	75.47 (1)	110 (22)	11.4 (4)
78.3 (2)	-	8.7 (15)	15/2	78.16 (1)	100 (29)	6.3 (3)
79.7 (2)	-	1.9 (5)	15/2	79.68 (4)	160 (90)	1.14 (17)
82.7 (2)	-	16.4 (19)	13/2	82.61 (1)	104 (23)	17.9 (6)
84.2 (2)	-	0.53 (25)	15/2	84.05 (5)	62 (67)	1.48 (22)
85.4 (2)	-	39.5 (40)	13/2	85.07 (2)	88 (30)	9.6 (5)
89.4 (3)	-	13.4 (25)	13/2	89.52 (2)	83 (33)	8.9 (5)
92.4 (3)	-	19.2 (21)	15/2	92.39 (1)	77 (26)	20 (2)
95.6 (3)	-	5.0 (13)	13/2	95.64 (2)	152 (58)	5.9 (4)
98.9 (3)	-	10 (3)	13/2	98.89 (2)	67 (39)	17 (5)
-	-	-	13/2	102.94 (9)	64 (62)	1.2 (3)
-	-	-	15/2	103.99 (15)	79 (69)	1.0 (8)
-	-	-	15/2	104.38 (8)	84 (72)	3.5 (10)
104.7 (4)	-	11 (4)	15/2	105.20 (5)	93 (73)	4.1 (5)
-	-	-	13/2	106.99 (6)	98 (73)	9.2 (15)
-	-	-	13/2	107.63 (6)	81 (74)	9.8 (15)
108.6 (4)	-	21 (7)	13/2	108.94 (5)	101 (57)	9.1 (10)
112.6 (5)	-	7 (3)	15/2	112.66 (3)	127 (54)	7.6 (5)
-	-	-	15/2	115.12 (3)	105 (57)	5.9 (4)

122.2 (5)	-	2.3 (10)	15/2	122.5 (1)	72 (71)	2.1 (5)
124.1 (5)	-	9.4 (43)	15/2	124.33 (3)	74 (40)	11.4 (7)
126.4 (5)	-	10.5 (45)	13/2	126.60 (4)	55 (54)	7 (3)
-	-	-	13/2	132.21 (13)	81 (67)	6 (2)
-	-	-	13/2	132.87 (15)	107 (83)	7 (3)
133.5 (6)	-	135 (15)	13/2	133.62 (15)	104 (83)	19 (9)
-	-	-	13/2	134.18 (7)	115 (80)	46 (14)
135.4 (6)	-	59 (10)	15/2	135.9 (3)	154 (49)	56 (4)

TABLE III: Some new resonance parameters for ^{176}Lu(n,γ) up to 400 eV with their parameters optimized with the SAMMY code.

This work							
J	Energy (eV)	Γ_γ (meV)	$2g\Gamma_n$ (meV)	J	Energy (eV)	Γ_γ (meV)	$2g\Gamma_n$ (meV)
15/2	141.84 (4)	97 (68)	6.9 (6)	13/2	245.2 (2)	74 (67)	8 (3)
15/2	146.9 (1)	82 (82)	1.6 (4)	15/2	246.6 (4)	84 (75)	2 (1)
15/2	147.89 (5)	70 (62)	6.6 (7)	15/2	247.5 (1)	88 (79)	30 (10)
13/2	154.5 (2)	80 (74)	2.2 (8)	15/2	250.0 (1)	89 (85)	20 (5)
15/2	155.4 (1)	109 (91)	4.1 (6)	13/2	252.4 (1)	112 (88)	40 (11)
13/2	157.51 (3)	99 (48)	25 (2)	15/2	256.0 (2)	109 (86)	11 (2)
13/2	161.64 (4)	108 (70)	14.3 (14)	15/2	260.7 (1)	127 (76)	35 (8)
13/2	162.9 (3)	104 (92)	1.1 (6)	15/2	269.0 (4)	114 (1023	3 (2)
15/2	166.15 (4)	102 (74)	14 (2)	15/2	271.6 (1)	76 (64)	27 (9)
15/2	168.49 (10)	94 (87)	9 (2)	13/2	274.5 (2)	81 (75)	11 (2)
15/2	169.3 (2)	97 (78)	4 (2)	15/2	277.3 (1)	76 (79)	9 (2)
13/2	170.2 (3)	78 (70)	0.8 (6)	13/2	282.0 (3)	88 (80)	6 (2)
13/2	172.7 (1)	80 (71)	2.4 (5)	15/2	288.6 (2)	137 (106)	12 (2)
13/2	176.0 (2)	78 (70)	1.5 (5)	13/2	294.3 (2)	106 (94)	12 (3)
13/2	180.5 (2)	89 (73)	2.3 (6)	15/2	297.5 (4)	107 (96)	0.4 (4)
13/2	182.4 (3)	80 (72)	0.8 (5)	13/2	299.8 (2)	105 (98)	27 (12)
13/2	184.84 (4)	73 (46)	48 (28)	13/2	300.9 (2)	107 (93)	16 (4)
15/2	187.2 (3)	107(100)	1.4 (8)	13/2	304.2 (2)	118 (92)	36 (7)
15/2	188.44 (8)	83 (85)	9 (1)	13/2	308.4 (2)	103 (86)	21 (5)
13/2	191.10 (8)	78 (62)	19 (2)	15/2	310.7 (1)	117 (88)	35 (9)
13/2	193.5 (2)	91 (88)	2.8 (8)	13/2	315.4 (4)	81 (72)	5 (2)
13/2	197.5 (2)	92 (87)	2.3 (1)	13/2	321.1 (4)	80 (72)	2.2 (18)
15/2	199.09 (7)	92 (88)	11.9 (2)	13/2	326.0 (4)	80 (72)	1.8 (11)
15/2	203.76 (8)	92 (84)	14 (2)	13/2	331.4 (3)	90 (81)	12 (4)
13/2	205.3 (2)	100 (89)	6.4 (15)	13/2	339.2 (2)	59 (53)	13 (11)
13/2	209.71 (7)	87 (64)	27 (7)	13/2	341.8 (4)	61 (54)	8 (4)
13/2	213.2 (2)	100 (89)	16 (5)	13/2	345.3 (4)	70 (63)	2.3 (22)
15/2	214.00 (3)	87 (80)	4 (2)	13/2	349.5 (3)	72 (65)	23 (9)
15/2	214.5 (2)	126 (118)	10 (3)	13/2	352.4 (2)	102 (84)	44 (17)
15/2	216.5 (3)	118 (110)	3 (1)	13/2	358.2 (1)	107 (88)	52 (20)
13/2	218.2 (1)	106 (86)	25 (5)	13/2	362.1 (4)	88 (80)	12 (4)
15/2	219.3 (3)	106 (96)	2.9 (15)	13/2	364.9 (5)	80 (72)	0.30 (26)
15/2	221.1 (2)	93 (79)	14 (2)	13/2	367.3 (4)	87 (75)	10 (4)
15/2	222.0 (2)	111 (97)	3 (1)	13/2	370.3 (2)	102 (81)	34 (11)
15/2	227.29 (9)	135 (104)	15 (2)	13/2	375.7 (3)	105 (84)	30 (9)
13/2	233.4 (1)	107 (88)	24 (6)	13/2	379.5 (2)	122 (104)	51 (16)
15/2	235.3 (1)	91 (88)	9 (2)	13/2	387.5 (3)	94 (76)	18 (6)
15/2	237.6 (1)	96 (88)	10 (2)	13/2	393.3 (2)	106 (71)	76 (38)
15/2	239.0 (1)	100 (93)	11 (3)	13/2	403.1 (3)	104 (85)	34 (16)

TABLE IV: Reference input D_0 from different level densities models in RIPL2. [46]

Models	D_0 values
Back-Shifted Fermi Gas Model (BSFG)	(2.75±0.85) eV
Gilbert-Cameron Model	(2.75±0.85) eV
Generalized Super-Fluid Model (GSFM)	(2.57±0.85) eV
Level Spacings compilation [47]	(2.75±0.85) eV
This work	(2.20±0.02) eV

TABLE V: Some new resonance parameters for ^{176}Lu(n,γ) from 400 eV to 900 eV with only energy indication as uncertainties for resonance parameters are too large.

This work		
Energy (eV)		
402.3 (2)	554.8 (5)	698.0 (9)
412.0 (2)	566.1 (4	706.6 (9)
421.9 (5)	571.5 (5)	716.9 (5)
431.2 (3)	579.1 (3)	727.9 (7)
434.9 (5)	584.6 (5)	734.9 (6)
442.0 (4)	593.1 (8)	749.4 (7)
447.8 (2)	602.7 (8)	759 (1)
452.9 (6)	614.3 (4)	770.2 (7)
460.2 (4)	620.4 (8)	773.8 (9)
464.9 (3)	627.3 (6)	785.9 (9)
471.0 (2)	635.8 (6)	791.2 (6)
481.4 (5)	602.7 (8)	800.42 (3)
484.8 (5)	614.3 (4)	810.32 (2)
491.8 (6)	620.4 (8)	816.3 (9)
503.3 (6)	627.3 (6)	822.31 (2)
507.9 (4)	635.8 (6)	831.6 (7)
513.3 (7)	642.3 (5)	846.2 (9)
521.2 (3)	649.0 (5)	855.2 (8)
527.0 (7)	658.0 (5)	868.4 (3)
536.3 (3)	668.4 (8)	875.8 (9)
543.9 (3)	678.4 (5)	885.3 (9)
549.8 (7)	687.7 (7)	906 (1)

TABLE VI: Maxwellian-averaged cross section given in mb for various kT values for ^{176}(n,γ) reaction.

kT (keV)	ENDF/B-VII.1	This work+[5]+ENDF/B-VII.1 [30]	Ref. [5]	Percentage of resonance region
8	3243	3665±30	3586±62	20.6%
10	2829	3161±22	3109±44	15.8%
15	2230	2445±13	2421±27	9.6%
20	1903	2060±9	2046±20	6.6%
25	1694	1815±6	1806±17	4.8%
30	1540 [49]	1647±5	1639±14	3.8%

TABLE VII: Details of Maxwellian-averaged cross sections given in mb for various kT values for ^{176}Lu(n,γ) reaction. Three integrals, I1 [0-3keV], I2 [3keV-225keV], I3 [225keV-20MeV], are determined from the measurements of this work for I1 compared to the previous one given by K. Wisshak *et al*. [5], from [5] for I2 and from ENDF/BVII.1, JEFF3.2 and BRC for I3.

kT (keV) Neutron energy range	This work I1 [0-3keV]	I1 [5] [0-3keV]	I2 [5] [3keV-225keV]	I3 ENDF-BVII.1 [30] [225keV-20MeV]	I3 JEFF3.2 [31] [225keV-20MeV]	I3 BRC [32] [225keV-20MeV]
8	754±16	675±34	2911±25	0	0	0
10	502±11	450±22	2659±19	0	0	0
15	235±5	211±11	2210±12	0	0	0
20	136±3	122±6	1924±8	0.1	0.8	0.2
25	88±2	79.5±4.0	1726±6	1	4	1.4
30	62±2	55.8±2.8	1581±5	4	13	5
40	35±1	31.8±1.6	1371±4	19	46	23
50	23±1	20.6±1.0	1216±4	46	95	56
52	21.2±0.5	19.0±1.0	1189±3	53	105	64
60	16.0±0.4	14.4±0.7	1088±3	82	148	98
70	11.8±0.3	10.6±0.5	978±3	122	200	142
80	9.0±0.2	8.1±0.4	882±3	161	246	186
90	7.1±0.2	6.4±0.3	797±2	197	284	226
100	5.8±0.2	5.2±0.3	723±2	230	316	262